Comparison of Fundamental Radar Features for Differentiating Between Walking and Standing in Horizontal and Vertical Movement Directions

Muhammad Adi Nurhidayat[1] , Istiqomah[1,2]* , Fiky Yosef Suratman[1,2]

[1] School of Electrical Engineering, Telkom University, Bandung 40257, Indonesia
[2] The University Center of Excellence Intelligent Sensing-IoT, Telkom University, Bandung 40257, Indonesia

Corresponding Author Email: Istiqomah@telkomuniversity.ac.id

ABSTRACT

This study investigates the feasibility of using a basic 24 GHz one-dimensional (1D) radar for Human Activity Recognition (HAR), focusing on differentiating between walking and standing movements. We evaluate the radar's performance using various machine learning models, including K-means, GMM, SVM, and LSTM. Using the silhouette score and the Davies-Bouldin index, we evaluate the intra- and interclass results of K-means and GMM, while SVM and LSTM are used to analyze their performance. The results indicate that the LSTM model achieves high accuracy in both vertical and horizontal dimensions, with precision, recall, and F1-scores all above 98% for both standing and walking movements. However, the SVM model faces challenges in horizontal movement detection, consistent with the unsupervised learning results where the inter-class and intra-class distances for the horizontal dimension are not significant, making differentiation difficult. These findings delineate the boundaries and capabilities of a lower-specification radar for HAR, providing insights into its practical applications and limitations.

1. INTRODUCTION

In recent years, radar technology has significantly advanced, contributing to the monitoring and analysis of object movements in various contexts [1-6]. While most research in Real-Time Human Activity Recognition (HAR) has focused on high-specification, multi-dimensional radar systems, the feasibility of using lower-specification, cost-effective radars remain underexplored [1].

Identifying and separating object movements is crucial in applications such as Navigation, Security Monitoring, and Human Activity Recognition. Studies emphasize that preprocessing radar data is essential before using it in generalization methods, such as filtering or eliminating static object reflections [2-4]. Additionally, the direction of object movement relative to the radar's point of view during data collection significantly affects the resulting movement pattern and the accuracy of activity detection. Both vertical and horizontal movements fall under this direction, and they have an impact on how well machine learning algorithms detect human movements.

Walking and standing movements have distinct characteristics. Walking involves continuous transitions between adjacent positions, while standing refers to an object remaining in a fixed position. Differentiating these two types of movement is vital for applications like intrusion detection and monitoring human movement in security scenarios.

This study aims to investigate whether a basic 24 GHz one-dimensional (1D) radar can effectively differentiate between walking and standing movements, particularly when analyzed in both vertical and horizontal dimensions. In real-time HAR, much research focuses on multi-dimensional radar systems or radars with frequencies exceeding 60 GHz [5, 6]. Radar systems vary significantly: 1D radars capture range, 2D radars capture range and azimuth, and 3D radars capture range, azimuth, and altitude. Thus, 1D radar is considered an inferior variant compared to 2D and 3D radars because it only captures range data [1].

We give a comparative analysis of 1D radar's capacity to distinguish between walking and standing movements using several techniques in order to overcome this difficulty. We extract range information to capture the Doppler effect and apply K-means, Gaussian Mixture Model (GMM), Support Vector Machine (SVM), and Long Short-Term Memory (LSTM). K-means and GMM represent unsupervised learning approaches, while SVM and LSTM represent supervised learning approaches. We evaluate K-means and GMM using silhouette scores and the Davies-Bouldin index to assess intra-class and inter-class separation. SVM and LSTM are evaluated based on precision, recall, F1-score, and accuracy.

Our research aims to outline the capabilities and limitations of such a radar system in HAR, offering valuable insights into its potential applications. This analysis will help determine the effectiveness, accuracy limits, and performance boundaries of a 24 GHz 1D radar in recognizing human activities.

2. RESEARCH METHODS

Figure 1 illustrates the methodology used in this research, detailing the process from data collection to the analysis of movement from different radar perspectives. The raw in-phase and quadrature (IQ) radar data acquired undergoes several preprocessing stages before being fed into the machine learning framework. Initially, the IQ data is scaled using a Digital-to-Analog Converter (DAC). Following this, DC removal is performed to eliminate any direct current (DC) components present in the data. Subsequently, clutter removal filters out low-frequency data and static object reflections, reducing noise in the signal. The next step involves applying the Fast Fourier Transform (FFT) to extract distance information, followed by the Short-Time Fourier Transform (STFT) to capture the Doppler effect and analyze movement.

After preprocessing, the data is processed through the machine learning stage, which employs both unsupervised and supervised learning techniques. Unsupervised learning identifies patterns and structures in the data without prior labels. Supervised learning evaluates the model's performance in distinguishing between vertical and horizontal movements. This comprehensive methodology ensures accurate and reliable detection of movement, leveraging the capabilities of a 24 GHz one-dimensional radar system.
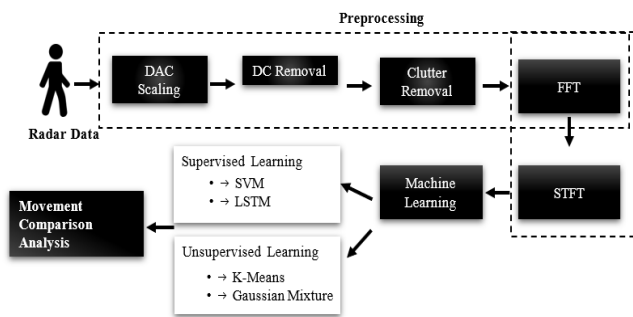
Figure 1. Proposed method

2.1 Radar

In this study, we used the uRad 24 GHz Radar operating in FMCW (Frequency-Modulated Continuous Wave) mode [7]. This radar measures the frequency shift of microwaves reflected by moving objects, allowing for accurate distance measurements. As a one-dimensional radar, it captures range data effectively.

We configured the radar to operate at 30 frames per second (FPS) for adequate data acquisition and set it to record 50 scans (Ns) to ensure comprehensive data collection. The radar's bandwidth was set to 200 MHz to optimize sensitivity to distance changes. With these settings, the radar can detect human movement up to 15.692 meters [7].

The formula used to determine the maximum distance from the radar is provided in Eq. (1):

$$Distance_{max} = 75 \times \frac{Ns}{BW} \qquad (1)$$

2.2 Data acquisition

The data collection process involved the careful placement of a 24 GHz FMCW radar relative to the subject. The radar was positioned at a height of 1 meter and placed 1.5 meters away from the detection zone, which was marked with black lines, as illustrated in Figures 2 and 3. This setup ensured that the subject's position and movements were within the radar's detection range. Only one subject participated in the research. The subject performed walking and standing movements in both vertical and horizontal dimensions for 300 seconds (about 5 minutes) walking and 30 seconds for standing at predefined points. This experimental setup ensured consistent data acquisition for both types of movements, enabling an analysis of the radar's performance in different scenarios.
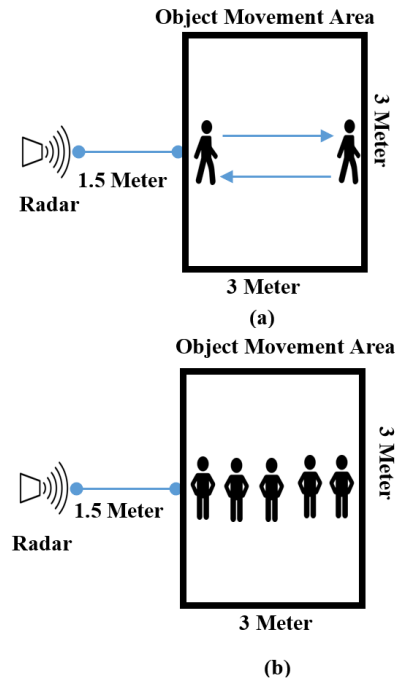
Figure 2. Radar position and object movement vertical: (a) Walking movement pattern vertically; (b) Standing movement pattern vertically
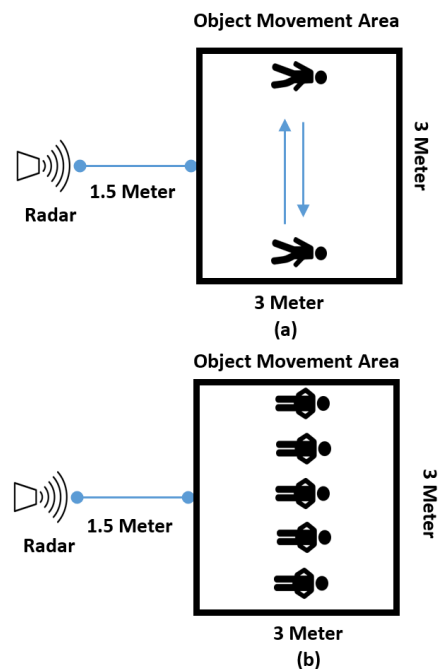
Figure 3. Radar position and object movement horizontal: (a) Walking movement pattern horizontally; (b) Standing movement pattern horizontally

2.3 Preprocessing

2.3.1 DAC scaling

In the preprocessing stage, the DAC scaling process is performed to convert the data from arbitrary units to more meaningful voltage units. The data provided by uRad has a width of 12 bits, with a range of 0-4095 [8]. Eq. (2) shows how the DAC process takes place.

$$V_{ADC} = \frac{X_{ADC}}{intervals} \times V_{ref} \qquad (2)$$

where, X in the equation presents the value of $I + jQ$ for each data. While V_{ref} represents the GPIO voltage provided by the Raspberry Pi 4 model B, which is 3.3 V [9].

2.3.2 DC removal

DC removal eliminates the continuous current component that may be present in the data after conversion to the analog domain. This step is crucial to ensure that static or constant signals do not interfere with the analysis.

For this process itself is shown by Eq. (3), where N_s is a radar signal with a number of samples.

$$y_{Ns} = X_{Ns} - \frac{1}{N_s} \sum_{n=0}^{Ns-1} x_{Ns}[n] \qquad (3)$$

The mean value of the signal is subtracted from each data point, ensuring the data is zero-centered and free from static interference [10, 11].

2.3.3 Clutter removal

After we conduct the DC removal process, the next step will be the clutter removal process. The main purpose of this step is to remove unwanted interference or noise from radar data that can obscure relevant information related to object movement.

Clutter, or interference, can come from signals reflected by irrelevant objects, such as walls, ground, or other objects that are not the main focus of the research. The typical clutter removal process involves using a high-pass filter or subtracting a reference signal that represents the clutter. One common approach is to subtract the mean (or average) of the signal over time, assuming that clutter is relatively constant and the mean captures the clutter component. Eq. (4) shows how the clutter removal process is done.

$$y_{Ns} = X_{Ns} - \frac{1}{Ns} \left[\sum_{n=0}^{Ns-1} x_{Ns}[n] \right]^T \qquad (4)$$

2.3.4 FFT

In order to convert time-domain signals into the frequency domain and help identify the frequency components present in the data, the Fast Fourier Transform (FFT) approach is frequently employed in signal analysis. Following the completion of all data cleaning procedures, FFT is applied.

In the case of FMCW radar, this process converts radar data that was originally in the voltage and time dimensions into the distance and time dimensions. Figure 4 shows the results of the spectrogram of the activities of a person walking vertical and horizontal, x is representing the time and y is representing the range. If you notice the Figure 4(a), you can see that person

is walking at a fast pace toward the radar and away from the radar. While Figure 4(b) shows the signal of the radar a range the same, it happens because radar data only capture the range, so when you are walking horizontally the differences in range are not very visible, so the signal looks similar. The equation for the FFT process itself is shown by Eq. (5), where k in Eq. (5) indicates the frequency index (k=0, 1, 2, …, K-1) and N_s the number of samples [12, 13].

$$X[k] = \sum_{n=0}^{N_S-1} x_{N_S}[n] e^{-j2\pi \frac{n}{N_S}[k]} \qquad (5)$$
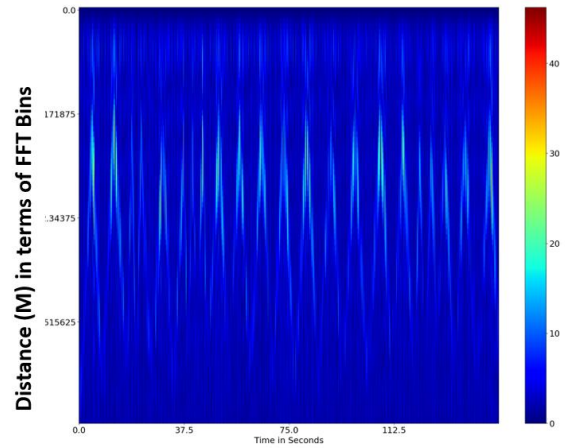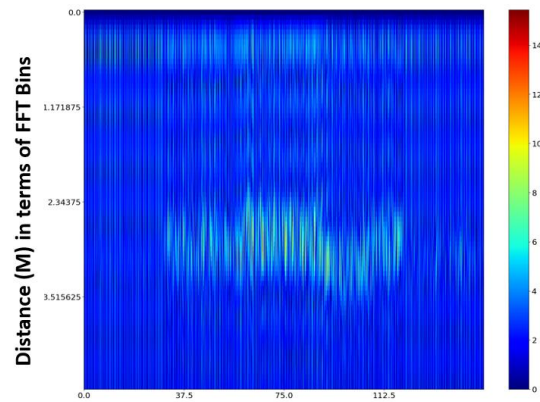
Figure 4. Range-time spectrogram of FFT results, (a) Vertical; (b) Horizontal

2.3.5 STFT

Next, after FFT, we will proceed to the STFT process to obtain doppler information. STFT is almost similar to FFT, except that the FFT in the STFT process is performed using Windowing. There are many types of windowing that can be used, such as Rectangular, Hamming, Hanning, and Blackman. Eq. (5) shows the equation for the STFT process. To obtain micro-doppler data, STFT is performed at the same distance with different times [14, 15].

$$X[k,m] = \sum_{n=0}^{N-1} x[n]w[n+mH] e^{-j2\pi \frac{n}{N_S}[k]} \qquad (6)$$

Radar data that was originally 2-dimensional, namely

range-time data, is now 3-dimensional, namely range-doppler-time, as shown in Figures 5 and 6, frame at the image is representing bin time, while x is range and y is frequency.

Before entering the classification process, the data is formed into a Windowed dataset, where 1 Windowed dataset consists of 60 samples.
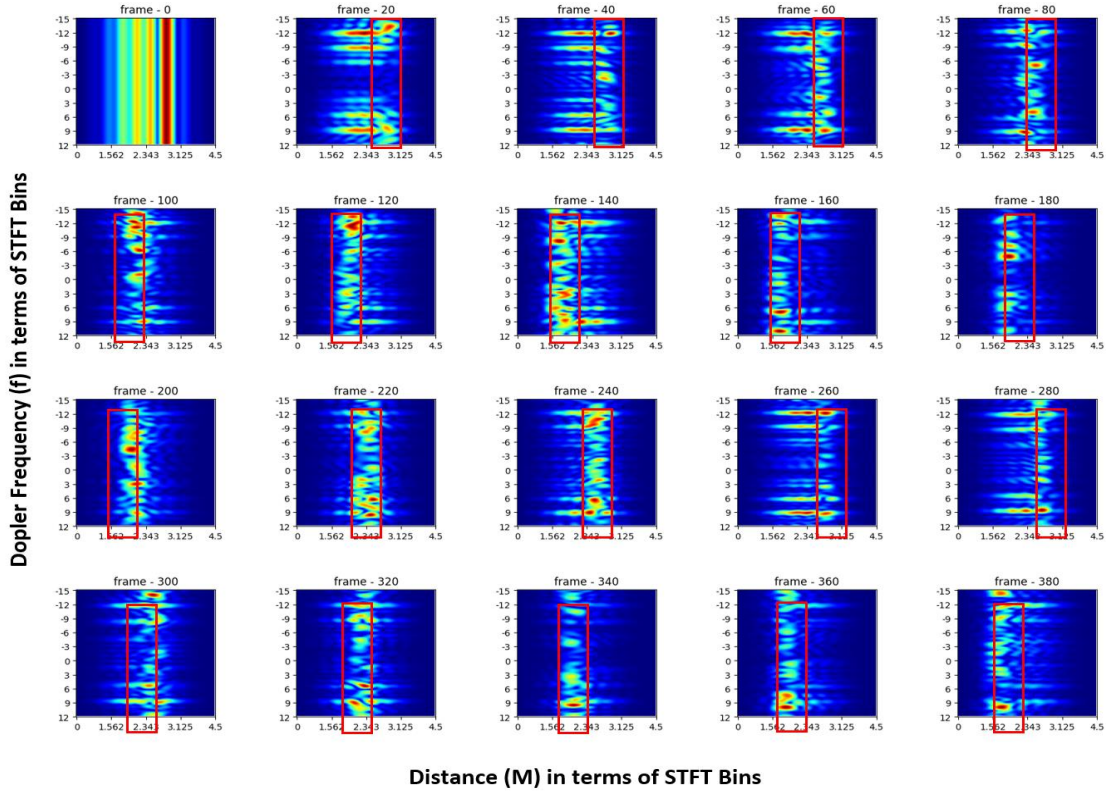
Figure 5. STFT result transition vertical movement
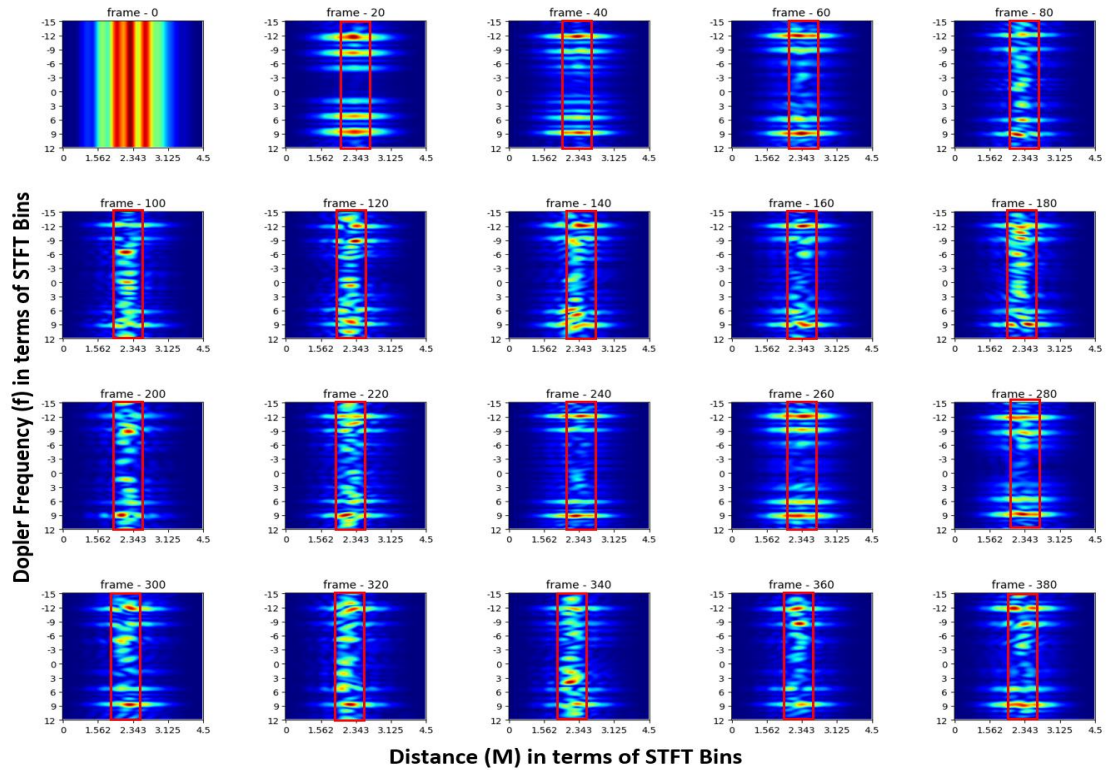
Figure 6. STFT result transition horizontal movement

2.4 Machine learning

2.4.1 Unsupervised learning

Unsupervised learning plays a crucial role in calculating the

distance between inter and intra-class data points. Two popular unsupervised learning algorithms used for this purpose are K-means and Gaussian Mixture Model (GMM). For this, two well-liked unsupervised learning methods are employed:

Gaussian Mixture Model (GMM) and K-means. The Euclidean distance metric is used by the K-means clustering method to categorize data points according to their proximity [16]. However, by adding a probabilistic model that presupposes data points are produced from a mixture of Gaussian distributions, GMM expands on the idea of K-means [17]. This allows GMM to capture more complex data patterns compared to K-means.

Metrics like the Davies-Bouldin index and silhouette score are frequently used to assess the quality of clustering findings. With values ranging from -1 to 1, the silhouette score indicates how similar an object is to its cluster in relation to other clusters. Better-defined clusters are indicated by a higher silhouette score. The Davies-Bouldin index, on the other hand, measures the average similarity between each cluster and its most comparable cluster; lower values denote better clustering outcomes [18].

$$s(i) = \frac{b(i) - a(i)}{max\,(a(i), b(i))} \qquad (7)$$

The silhouette score for a given data point can be found using Eq. (7). $a(i)$ is the average distance from i to all other data points in the same cluster. This represents the intra-class similarity. an than $b(i)$ is the smallest average distance from i to all data points in any other cluster, calculated for each cluster. This represents the inter-class dissimilarity. To measure the silhouette score for the entire dataset, you can use Eq. (8).

$$S = \frac{1}{n}\sum_{i=1}^{n} s(i) \qquad (8)$$

The Davies-Bouldin index can be calculate through the Eq. (9):

$$DBI = \frac{1}{K}\sum_{i=1}^{K} \max_{i,j\neq i} \frac{S_i + S_j}{d_{i,j}} \qquad (9)$$

where, $S_i = \frac{1}{|C_i|}\sum_{x_j\in C_i}\|x_j - v_i\|$ is the measure of dispersion within cluster i, K is the number of clusters, x_j is an n-dimensional feature vector assigned to cluster i, v_i is the centroid of cluster i, C_i represents cluster i, $\| \bullet \|$ is the Euclidean distance, $d_{i,j}=\|v_i-v_j\|$ is the Euclidean distance i and j [19, 20].

In the context of machine learning tasks like classification, the variability within and between classes significantly impacts model performance. High interclass variability and low intraclass variability are generally preferred for classification tasks as they facilitate better class separation. However, in certain scenarios, high intraclass variability may be necessary for capturing subtle differences within a class, especially when dealing with complex datasets [21].

2.4.2 Supervised learning

A key part of machine learning is supervised machine learning, in which algorithms are trained on labeled data in order to generate predictions or judgments. One popular algorithm used in supervised learning is the Support Vector Machine (SVM). SVM is an effective classifier that searches a high-dimensional feature space for the ideal hyperplane to divide various classes [22]. The core idea behind SVM is to address linear inseparability through the kernel formula and then determine the optimal classification surface using convex quadratic programming [23]. SVMs are useful tools for resolving machine learning issues since they have their roots in statistical learning theory and optimization techniques [24].

On the other hand, LSTM, a special type of Recurrent Neural Network (RNN), is known for its ability to solve complex tasks with long-time dependencies and predict chaotic dynamical systems with stability [25, 26]. LSTM networks are made up of memory cells with a lengthy retention time, which enables them to retain and forget information as needed. The input gate, forget gate, output gate, and memory cell are essential parts of an LSTM unit that cooperate to control the information flow across the network [27].

As we know, supervised learning like SVM and LSTM is used for classification algorithms, but in this research, these two algorithms will be mainly used to see the performance of models whose data patterns differ vertically and horizontally.

3. RESULT AND ANALYSIS

Figures 5 and 6 display the spectrograms in 20 segments, ranging from 0 to 380 time bins. The red box in the figures represents the presence of a person. It is evident that vertical movements are more easily discernible than horizontal ones. To further analyze this, we applied the previously discussed algorithms, starting with unsupervised learning followed by supervised learning.

Before applying the unsupervised algorithms, we conducted Principal Component Analysis (PCA) to address the higher dimensionality of radar data. PCA reduces the data dimensions, making it more suitable for unsupervised learning. For vertical movement data, PCA reduced the original size from (1196, 355740) to (1196, 911). Similarly, for horizontal movement data, the dimensions were reduced from (1196, 355740) to (1196, 974).

Based on Table 1, it can be concluded that the radar is more effective in identifying vertical movements than horizontal movements. Both the K-means and Gaussian Mixture Model (GMM) methods provide consistent results in both dimensions. The silhouette scores and Davies-Bouldin indices indicate that vertical movements are easier to differentiate, showing better intra-class and inter-class separation compared to horizontal movements. The analysis suggests some overlap or difficulty in clearly separating walking and standing movements, likely due to the limitations of a 1D radar that only captures range.

Table 2 presents the performance metrics for various supervised machine learning models. Among them, the LSTM model excelled with the highest precision, recall, and accuracy in both horizontal and vertical dimensions. This indicates its superior capability in maintaining long-term dependencies and accurately predicting movement patterns. Conversely, the SVM model performed poorly in horizontal movements, which is consistent with the unsupervised learning results. This is because SVM uses a hyperplane to separate classes, which is less effective when inter- and intraclass distances are small. Li et al. [28] reported a 92% accuracy with adaptive thresholding methods, but our LSTM model surpassed this with a 99% accuracy. Specifically, the SVM model performed better in the vertical dimension than in the horizontal dimension, achieving 62% precision, 70% recall, and 66% F1-score for standing, and 64% precision, 56% recall, and 65% F1-score for walking.

Table 1. Evaluation of data distribution with K-means clustering and GMM

	Vertical Movement	Horizontal Movement
K-Means Silhouette Score	0.32	0.15
K-Means Davies-Bouldin Index	1.72	2.38
GMM Silhouete Score	0.32	0.15
GMM Davies-Bouldin Index	1.72	2.38

Table 2. Evaluation of supervised learning (SVM and LSTM)

SVM (Support Vector Machine) Model						
	Vertical			**Horizontal**		
	Precision	**Recall**	**F1-Score**	**Precision**	**Recall**	**F1-Score**
Standing	0.98	0.99	0.98	0.62	0.70	0.66
Walking	0.99	0.97	0.98	0.64	0.56	0.65
Accuracy			0.98			0.63
LSTM (Long-Short Term Memory) Model						
	Vertical			**Horizontal**		
	Precision	**Recall**	**F1-Score**	**Precision**	**Recall**	**F1-Score**
Standing	0.99	1.00	1.00	0.99	0.98	0.99
Walking	1.00	0.99	1.00	0.98	0.99	0.99
Accuracy			1.00			0.99

(a)
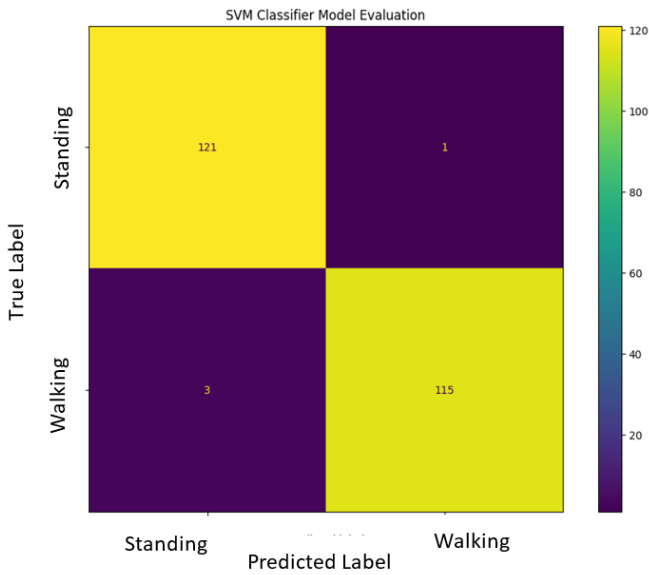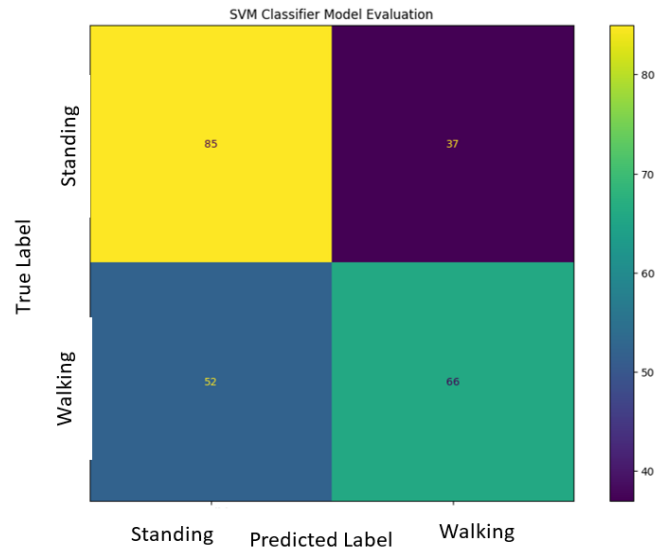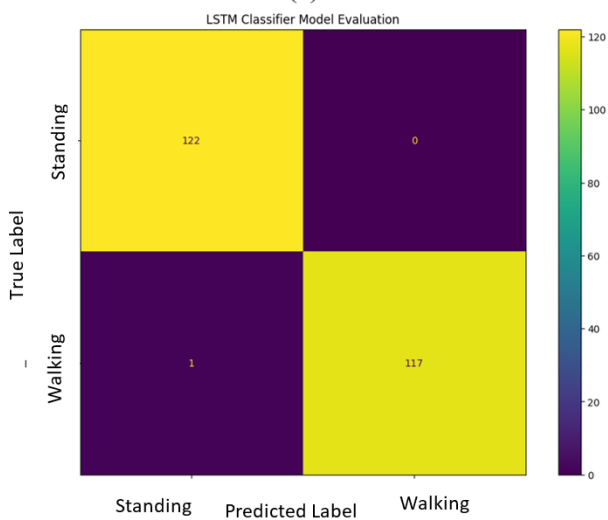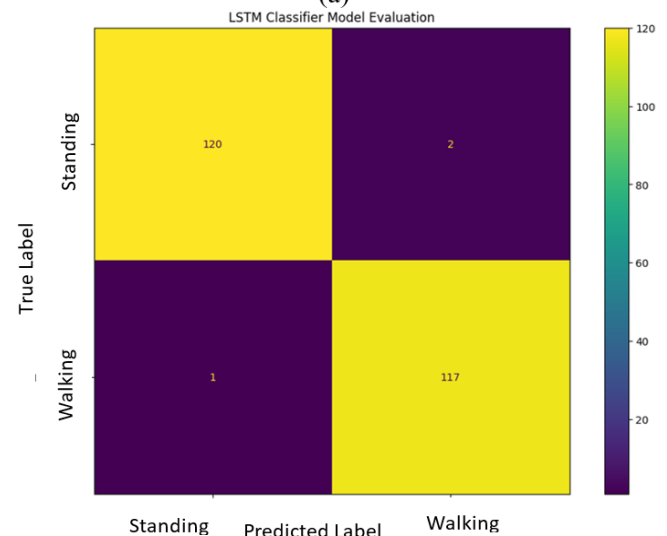
(b)

Figure 7. Heatmap for vertical movement: (a) SVM; (b) LSTM

(a)

(b)

Figure 8. Heatmap for horizontal movement: (a) SVM; (b) LSTM

To confirm the findings in Table 2, we developed heatmaps illustrated in Figures 7 and 8. The vertical dimension heatmap in Figure 7 aligns with Table 2, showing that both SVM and LSTM perform well. In contrast, the horizontal dimension heatmap in Figure 8 indicates that the SVM algorithm produces poorer results than the others, as reflected in the high number of false positives and false negatives. This difficulty arises because the interclass and intraclass data points are too closely positioned, hindering SVM's ability to differentiate between them. In comparison, the Long Short-Term Memory (LSTM) model benefits from its advanced architecture, which includes memory cells to retain historical information, thereby achieving significantly greater accuracy.

4. CONCLUSIONS

This study investigated the use of a 24 GHz one-dimensional (1D) radar for Human Activity Recognition (HAR) by differentiating between walking and standing movements in both vertical and horizontal dimensions. Outperforming the Support Vector Machine (SVM) model, the Long Short-Term Memory (LSTM) model scored the greatest accuracy for both vertical and horizontal motion detection (100% and 99%). However, according to the results from unsupervised learning reinforced by the results from the SVM radar system, the 1D radar showed limitations in effectively separating walking and standing movements in the horizontal dimension. This suggests the need for higher-dimensional radar systems or advanced data processing techniques. Despite these limitations, the high accuracy of the LSTM model indicates potential applications for cost-effective HAR systems using 24 GHz 1D radar. Future research should focus on real-world deployment and optimizing performance on hardware with limited computational power, such as microcomputers like the Raspberry Pi. Overall, the study highlights both the potential and limitations of low-specification radars for HAR.

ACKNOWLEDGMENT

REFERENCES

[1] Li, X., He, Y., Jing, X. (2019). A survey of deep learning-based human activity recognition in radar. Remote Sensing, 11(9): 1068. https://doi.org/10.3390/rs11091068

[2] Gupta, A., Gupta, K., Gupta, K., Gupta, K. (2020). A survey on human activity recognition and classification. In 2020 International Conference on Communication and Signal Processing (ICCSP), pp. 0915-0919. https://doi.org/10.1109/ICCSP48568.2020.9182416

[3] Kim, B., Kong, S.H., Kim, S. (2015). Low computational enhancement of STFT-based parameter estimation. IEEE Journal of Selected Topics in Signal Processing, 9(8): 1610-1619. https://doi.org/10.1109/JSTSP.2015.2465310

[4] Rafli, R., Suratman, F.Y., Istiqomah. (2023). FMCW Radar signal processing for human activity recognition with convolutional neural network. In Proceeding of the 3rd International Conference on Electronics, Biomedical Engineering, and Health Informatics: ICEBEHI 2022, Surabaya, Indonesia, pp. 429-445. https://doi.org/10.1007/978-981-99-0248-4_29

[5] Ullmann, I., Guendel, R.G., Kruse, N.C., Fioranelli, F., Yarovoy, A. (2023). A survey on radar-based continuous human activity recognition. IEEE Journal of Microwaves, 3(3): 938-950. https://doi.org/10.1109/JMW.2023.3264494

[6] Yang, Z., Wang, H., Ni, P., Wang, P., Cao, Q., Fang, L. (2021). Real-time human activity classification from radar with CNN-LSTM network. In 2021 IEEE 16th Conference on Industrial Electronics and Applications (ICIEA), pp. 50-55. https://doi.org/10.1109/ICIEA51954.2021.9516401

[7] uRAD by Anteral. User Manual Raspberry Pi version Software SDK v1.1. https://urad.es/en/descargas/.

[8] Zhu, J.P., Chen, H.Q., Ye, W.B. (2020). Classification of human activities based on radar signals using 1D-CNN and LSTM. In 2020 IEEE International Symposium on Circuits and Systems (ISCAS), Seville, Spain, pp. 1-5. https://doi.org/10.1109/ISCAS45731.2020.9181233

[9] Ryoo, M., Rothrock, B., Fleming, C., Yang, H.J. (2017). Privacy-preserving human activity recognition from extreme low resolution. In Proceedings of the AAAI Conference on Artificial Intelligence, 31(1). https://doi.org/10.1609/aaai.v31i1.11233

[10] Kang, S.W., Jang, M.H., Lee, S. (2021). Identification of human motion using radar sensor in an indoor environment. Sensors, 21(7): 2305. https://doi.org/10.3390/s21072305

[11] Jahn, M., Wagner, C., Stelzer, A. (2010). DC-offset compensation concept for monostatic FMCW radar transceivers. IEEE Microwave and Wireless Components Letters, 20(9): 525-527. https://doi.org/10.1109/LMWC.2010.2056359

[12] Gurbuz, S.Z. (2020). Deep Neural Network Design for Radar Applications. Institution of Engineering and Technology.

[13] Heo, J., Jung, Y., Lee, S., Jung, Y. (2021) FPGA implementation of an efficient FFT processor for FMCW radar signal processing. Sensors, 21(19): 6443. https://doi.org/10.3390/s21196443

[14] Ahmed, S., Park, J., Cho, S.H. (2022). FMCW radar sensor based human activity recognition using deep learning. In 2022 International Conference on Electronics, Information, and Communication (ICEIC), Jeju, Republic of Korea, https://doi.org/10.1109/ICEIC54506.2022.9748776

[15] Numpy.org. numpy.kaiser. https://numpy.org/doc/stable/reference/generated/numpy.kaiser.html.

[16] Ali, Y.H., Mohsen, M. (2018). Reflections removal using K-Means clustering. Al-Nahrain Journal of Science, 21(3): 162-168. https://doi.org/10.22401/JNUS.21.3.19

[17] Xu, J., Luo, Q. (2021). Human action recognition based on mixed gaussian hidden Markov model. MATEC Web of Conferences, 336: 06004.

https://doi.org/10.1051/matecconf/202133606004

[18] Likas, A., Vlassis, N., Verbeek, J.J. (2003). The global k-means clustering algorithm. Pattern Recognition, 36(2): 451-461. https://doi.org/10.1016/S0031-3203(02)00060-2

[19] Xiao, J., Lu, J., Li, X. (2017). Davies Bouldin Index based hierarchical initialization K-means. Intelligent Data Analysis, 21(6): 1327-1338. https://doi.org/10.3233/IDA-163129

[20] Petrovic, S. (2006). A comparison between the silhouette index and the Davies-Bouldin index in labelling ids clusters. In Proceedings of the 11th Nordic Workshop of Secure IT Systems, pp. 53-64.

[21] Bishop, C. (2006). Pattern recognition and machine learning. Journal of Electronic Imaging, 16: 140-155. https://doi.org/10.1117/1.2819119

[22] Yamada, K., bin Wan Hamat, W.J., bin Ishak, H.M., Hashikura, K., Suzuki, T. (2019). Detection of anxiety expression from EEG analysis using support vector machine. ECTI Transactions on Electrical Engineering, Electronics, and Communications, 17(1): 87-94. https://doi.org/10.37936/ecti-eec.2019171.215447

[23] Qiu, S., Wang, J., Gao, L. (2014). Discrimination and characterization of strawberry juice based on electronic nose and tongue: Comparison of different juice processing approaches by LDA, PLSR, RF, and SVM. Journal of Agricultural and Food Chemistry, 62(27): 6426-6434. https://doi.org/10.1021/jf501468b

[24] Tian, Y., Shi, Y., Liu, X. (2012). Recent advances on support vector machines research. Technological and Economic Development of Economy, 18(1): 5-33. https://doi.org/10.3846/20294913.2012.661205

[25] Kherad, M., Moayyedi, M.K., Fotouhi, F. (2021). Reduced order framework for convection dominant and pure diffusive problems based on combination of deep long short-term memory and proper orthogonal decomposition/dynamic mode decomposition methods. International Journal for Numerical Methods in Fluids, 93(3): 853-873. https://doi.org/10.1002/fld.4911

[26] Behera, A., Keidel, A., Debnath, B. (2018). Context-driven multi-stream LSTM (M-LSTM) for recognizing fine-grained activity of drivers. In German Conference on Pattern Recognition, pp. 298-314. https://doi.org/10.1007/978-3-030-12939-2_21

[27] Rahman, S.M., Pawar, S., San, O., Rasheed, A., Iliescu, T. (2019). Nonintrusive reduced order modeling framework for quasigeostrophic turbulence. Physical Review E, 100(5): 053306. https://doi.org/10.1103/PhysRevE.100.053306

[28] Li, Z., Le Kernec, J., Abbasi, Q., Fioranelli, F., Yang, S.F., Romain, O. (2023). Radar-based human activity recognition with adaptive thresholding towards resource constrained platforms. Scientific Reports, 13: 3473. https://doi.org/10.1038/s41598-023-30631-x